Brueckner-Bethe and variational calculations of nuclear matter

B. D. Day* and R. B. Wiringa
Physics Division, Argonne National Laboratory, Argonne, Illinois 60439
(Received 23 May 1985)

Results of both Brueckner-Bethe and variational calculations for the binding energy of nuclear matter as a function of density are presented for several recent nucleon-nucleon potentials. A detailed comparison is made for the Argonne v_{14} potential, the most realistic potential for which both methods have been used. The two methods agree reasonably well, with predicted saturation points of -17.8 MeV at 1.6 fm^{-1} for the Brueckner-Bethe method, and -16.6 MeV at 1.7 fm^{-1} for the variational method. The variational energies are 1—2 MeV above the Brueckner-Bethe energies for densities from 1.2 to 1.7 fm^{-1}. The results of Brueckner-Bethe calculations are also given for the Paris and Bonn potentials as well as results of variational calculations for the Urbana v_{14} potential. These potentials all give similar binding energy curves, and all saturate matter at a density significantly above the empirical value.

I. INTRODUCTION

Calculations of the binding energy as a function of density of symmetric nuclear matter have been made for many nucleon-nucleon potentials using either Brueckner-Bethe[1] or variational methods.[2] However, the most realistic potential for which both methods have been used to date is the Reid v_6 model,[3] a modification of the Reid soft-core potential[4] which includes central, spin, isospin, and tensor components but does not fit two-nucleon scattering data. The results for Reid v_6 indicated reasonable agreement between the two methods,[5,6] which represent rather different ways of solving the many-body Schrödinger equation. The variational calculation gave somewhat less binding near the empirical density (1.8 MeV less at $k_F=1.4$ fm^{-1}), but saturated at a higher density (1.7 instead of 1.6 fm^{-1}).

In this work we report results of both Brueckner-Bethe and variational calculations for the Argonne v_{14} potential,[7] a more sophisticated model than Reid v_6, which gives a good fit to nucleon-nucleon scattering data and deuteron properties. The agreement between the two methods is about the same as for the Reid v_6 model. We also present results of Brueckner-Bethe calculations for the Paris[8] and Bonn[9] potentials, and of variational calculations for the Urbana v_{14} potential.[2]

The nuclear Hamiltonian is taken as:

$$H=\sum_i(-\hbar^2/2m)\nabla_i^2+\sum_{i<j}v_{ij}\ . \tag{1}$$

The Argonne v_{14} potential is expressed as a sum of 14 operator components:

$$v_{ij}=\sum_{p=1,14}v_p(r_{ij})O_p(ij)\ , \tag{2}$$

where the operators $p=1,14$ are

$$O_p(ij)=1,\boldsymbol{\tau}_i\cdot\boldsymbol{\tau}_j,\boldsymbol{\sigma}_i\cdot\boldsymbol{\sigma}_j,(\boldsymbol{\sigma}_i\cdot\boldsymbol{\sigma}_j)(\boldsymbol{\tau}_i\cdot\boldsymbol{\tau}_j),S_{ij},S_{ij}(\boldsymbol{\tau}_i\cdot\boldsymbol{\tau}_j),\mathbf{L}\cdot\mathbf{S},\mathbf{L}\cdot\mathbf{S}(\boldsymbol{\tau}_i\cdot\boldsymbol{\tau}_j),L^2,L^2(\boldsymbol{\tau}_i\cdot\boldsymbol{\tau}_j),L^2(\boldsymbol{\sigma}_i\cdot\boldsymbol{\sigma}_j)\ ,$$
$$L^2(\boldsymbol{\sigma}_i\cdot\boldsymbol{\sigma}_j)(\boldsymbol{\tau}_i\cdot\boldsymbol{\tau}_j),(\mathbf{L}\cdot\mathbf{S})^2,(\mathbf{L}\cdot\mathbf{S})^2(\boldsymbol{\tau}_i\cdot\boldsymbol{\tau}_j)\ . \tag{3}$$

The Reid v_6 potential contains terms of type $p=1,6$ only. The additional L-dependent terms in Eq. (3) are required to give good fits to current scattering data. The Urbana v_{14} potential can be written in the same form. The parametrized version of the Paris potential also has the same operator structure except that p^2 is used instead of L^2.

The Brueckner-Bethe method has been used to study nuclear matter with a wide range of two-body potentials,[1] including the Reid soft-core, Paris, and Bonn potentials. However it has not been used to date for potentials like Argonne v_{14}. The variational method, using Fermi hypernetted chain and single operator chain summation techniques, has been developed specifically for potentials like Argonne v_{14} where the L-dependent terms are relatively weak. It has not been developed for potentials like the Reid soft core, which lacks a consistent operator structure, or Paris, which has a very strong p^2 dependence.[2] It also has not been applied to momentum-space potentials like the Bonn potential. Despite the limited range of two-body potentials it can currently be used for, it has been adapted for the study of three-body potentials[10] and also for the study of nuclear and neutron matter at high densities and finite temperatures.[11] The interesting con-

TABLE I. Separable representation used in various channels for the Brueckner-Bethe calculation of higher-order diagrams in D_3^c, for the Argonne v_{14} potential.

Channel	Separable representation	Channel	Separable representation
$^1S_0$	$2R+1A$	$^1P_1$	$3R$
$^3S_1$-$^3D_1$	$4R+3A$	$^3P_0$	$2R+2A$
$^1D_2$	$1A$	$^3P_1$	$3R$
$^3D_2$	$1R+1A$	$^3P_2$-$^3F_2$	$3R+3A$
$^3D_3$-$^3G_3$	$2R+2A$	$^1F_3$	$1R$
$^1G_4$	$1A$	$^3F_3$	$1R$
$^3G_4$	$1R$	$^3F_4$-$^3H_4$	$1A$
$^3G_5$-$^3I_5$	$1A$		

clusions drawn from these latter studies are dependent on the accuracy with which the variational method solves the basic nuclear matter problem. The present work tests this by comparison with the Brueckner-Bethe method.

II. BRUECKNER-BETHE CALCULATIONS

In the Brueckner-Bethe (BB) calculation the coupled-cluster equations have been solved in the hole-line approximation, including two-, three-, and four-hole-line contributions. The conventional single particle spectrum is used, i.e., kinetic energy above the Fermi sea and the Brueckner-Hartree-Fock (BHF) energy for states in the Fermi sea. We find that approximating the BHF spectrum by a quadratic causes negligible error in the calculated energy, so in practice we use the single-particle spectrum:

$$E(k)=k^2/2m^*-E_0\ ,\ (k<k_F)\ ,$$
$$k^2/2m\ ,\ (k>k_F)\ , \tag{4}$$

where m^* and E_0 are determined self-consistently from the equation

$$E(k)=k^2/2m+\sum_{l<k_F}(kl\mid G\mid kl)\ . \tag{5}$$

The reaction matrix G satisfies

$$G=V-V(Q/e)G\ , \tag{6}$$

where Q is the Pauli operator and e is the energy denominator determined from $E(k)$. The two-hole-line, i.e., two-body, contribution to the binding energy is given by:

$$D_2=\tfrac{1}{2}\sum_{k,l<k_F}(kl\mid G\mid kl)\ . \tag{7}$$

Calculating D_2 with a kinetic-energy spectrum above the Fermi sea amounts to neglecting the interaction of a particle above the sea with the other particles in the system. This interaction is taken into account by the three-body cluster term D_3^c, which is the dominant contribution to the three-hole-line energy D_3. It may also be possible to account for this interaction by using a modified single-particle potential above the Fermi sea. However, the only way to determine this potential is to do the same three-body calculation that gives D_3^c. Hence an accurate calculation of the three-body correlations is essential in any adequate approximation scheme. This crucial point is discussed further in Refs. 5 and 12.

The calculations have been done in momentum space and require as input, matrix elements of the potential $\langle kl\mid V(jST)\mid k'l'\rangle$. These can be calculated analytically for the Reid, Paris, and Bonn models. For the Argonne v_{14} potential they have been computed numerically by integration over r using Simpson's rule with the 400-point mesh:

0(0.0025)0.25(0.005)0.5(0.01)1.0(0.02)2.0(0.04)4.0(0.08)12.0 .

This mesh gives D_2 accurate to 0.001 MeV and D_3 and D_4 to 0.02 MeV. The computing time is comparable to that required for analytic evaluation of matrix elements using the Reid potential.

Once the matrix elements of V are available, the calculation of the two-body contribution D_2 is straightforward. D_3 and D_4 are calculated as described in Ref. 5, except that for two-body states in the Fermi sea we include only $l_0=0,1$ (S and P waves) rather than $l_0\leq 2$ (S, P, and D waves), as was done earlier. This changes the calculated energy by only 0.2 MeV at the highest density considered ($k_F=1.8$ fm^{-1}) and is thus an acceptable approximation.

As discussed in Ref. 5, D_3^c is given by

$$D_3^c=B+R+H\ , \tag{8}$$

where B and R are, respectively, the lowest-order bubble and ring diagrams, and H is the sum of all higher-order three-body cluster diagrams. The calculation of H makes

TABLE II. Self-consistent values of m^* and E_0 in the Brueckner-Bethe calculation for the Argonne v_{14} potential.

k_F (fm^{-1})	1.2	1.4	1.6	1.8
m^*/m	0.689	0.644	0.603	0.568
E_0 (MeV)	62.38	83.69	105.38	125.29

TABLE III. Partial-wave contributions to D_2 in MeV for the Argonne v_{14} and Paris potentials at $k_F=1.4$ fm^{-1}.

Channel	Argonne v_{14}	Paris
$^1S_0$	−17.16	−16.98
$^3S_1$	−17.63	−17.98
$^1P_1$	4.52	4.88
$^3P_0$	−4.11	−3.83
$^3P_1$	12.17	11.69
$^3P_2$	−7.65	−8.14
$^1D_2$	−3.17	−3.21
$^3D_1$	1.60	1.69
$^3D_2$	−4.62	−4.65
$^3D_3$	0.14	0.13
$l>3$	0.79	0.86
Total D_2	−35.12	−35.54

use of a separable representation of the off-shell reaction matrix:

$$(kl \mid G \mid k'l')=\sum_\beta g_\beta(kl)\lambda_\beta g_\beta(k'l') . \tag{9}$$

For the Argonne v_{14} potential the number of terms retained in each jST channel is given in Table I, where the notation $1R+2A$ means that one repulsive (positive) λ_β and two attractive (negative) λ_β's are retained. This truncation causes an error of about 0.25 MeV in the calculated energy at $k_F=1.8$ fm^{-1}, and the error decreases rapidly as k_F is lowered.

The values of m^* and E_0 obtained from the self-consistent two-body calculation are shown in Table II. $E(k)$ was first calculated for four equally spaced values of k from 0.25 k_F to k_F. Then m^* was chosen to reproduce the change of $E(k)$ between 0.5 k_F and k_F, and E_0 was chosen to correctly give the average of $E(k)$ over the Fermi sea. The partial-wave breakdown of D_2 at $k_F=1.4$ fm^{-1} is shown in Table III. For comparison, the corresponding results for the parametrized Paris potential are also shown, using $m^*/m=0.647$ and $E_0=84.39$ MeV. Table IV shows the contributions to the calculated energy, E_{BB}, for various values of k_F. The kinetic energy of the Fermi sea is denoted by T, and D_2, D_3, and D_4 are the two-, three-, and four-hole-line contributions. The uncertainty given for the total is estimated by the method of Ref. 5. The breakdown of the three-body cluster energy D_3^c into bubble, ring, and higher-order contributions is shown in Table V.

TABLE V. Bubble (B), ring (R), and higher-order (H) contributions in MeV/nucleon to the Brueckner-Bethe three-body cluster energy for the Argonne v_{14} potential.

k_F (fm^{-1})	1.2	1.4	1.6	1.8
B	−0.47	0.77	3.80	10.20
R	−1.49	−3.21	−5.82	−9.45
H	−0.95	−2.04	−4.10	−7.64
D_3^c	−2.91	−4.48	−6.12	−6.89

The wound parameter κ is defined by

$$\kappa=\sum_{\substack{k,l<k_F\\ a,b>k_F}} |(ab \mid S_2 \mid kl)|^2 , \tag{10}$$

where S_2 is the two-particle, two-hole amplitude in the exact many-body ground state. It is necessary to have $\kappa \ll 1$ for the hole-line expansion to be valid. The lowest-order approximation κ_2 is determined using the Bethe-Goldstone two-body wave function. An improved approximation κ_{GR} is obtained by summing the generalized ring (GR) series, which includes three-body correlations.[5] Table VI shows these two approximations to κ.

III. VARIATIONAL CALCULATIONS

The variational method[2,3] is used to compute an upper bound E_v to the ground-state energy E:

$$E_v(\lambda)=\langle\psi_v(\lambda) \mid H \mid \psi_v(\lambda)\rangle / \langle\psi_v(\lambda) \mid \psi_v(\lambda)\rangle \geq E . \tag{11}$$

Here λ denotes a set of parameters used in constructing the trial function ψ_v; the parameters are varied to minimize E_v and thus obtain the lowest upper bound on E. With a flexible choice for ψ_v and an accurate evaluation of the expectation value, E_v should be close to E.

The trial function is constructed as a symmetrized product of two-body correlation operators F_{ij} acting on the Fermi-gas wave function ϕ:

$$\psi_v(\lambda)=\left[S\prod_{i<j}F_{ij}(\lambda)\right]\phi . \tag{12}$$

We expect that the main correlations induced by the potential V_{ij} can be represented in an operator format similar to Eq. (2). For simplicity we use a truncated set of operator components,

TABLE IV. Contributions in MeV/nucleon to the Brueckner-Bethe energy for the Argonne v_{14} potential.

k_F (fm^{-1})	1.2	1.4	1.6	1.8
T	17.92	24.39	31.85	40.31
D_2	−27.14	−35.12	−42.21	−47.33
D_3	−3.12	−4.80	−6.59	−7.53
D_4	−0.48	−0.64	−0.84	−1.28
E_{BB}	−12.8±0.5	−16.2±0.9	−17.8±1.3	−15.8±2.0

TABLE VI. The two-body and generalized ring approximations to κ in the Brueckner-Bethe calculation for the Argonne v_{14} potential.

k_F (fm^{-1})	1.2	1.4	1.6	1.8
κ_2	0.101	0.118	0.144	0.178
κ_{GR}	0.190	0.196	0.220	0.25

TABLE VII. Variational parameters for the Argonne v_{14} potential.

k_F (fm^{-1})	1.2	1.4	1.6	1.7	1.8
d (fm)	2.41	2.18	2.05	2.17	2.14
d_t (fm)	4.82	4.35	4.09	3.85	3.81
α	0.70	0.62	0.56	0.53	0.50

$$F_{ij}(\lambda)=\sum_{p=1,8} f_p(r_{ij};d,d_t,\alpha)O_p(ij)\ , \tag{13}$$

which includes tensor and spin-orbit correlations, but neglects L^2 and $(\mathbf{L}\cdot\mathbf{S})^2$ correlations. The f_p's are generated by solving a set of eight coupled Euler-Lagrange equations which include all components of the potential and satisfy the boundary condition $F_{ij}(r\to\infty)=1$. The parameter set λ includes central and tensor healing distances, d and d_t, and a quenching factor α for noncentral interactions.[6]

The expectation value E_v is evaluated in a diagrammatic cluster expansion based on generalized Mayer diagrams.[3] The two-body cluster energy is calculated exactly, while three-body and higher-order cluster terms are calculated using the Fermi hypernetted chain—single operator chain (FHNC—SOC) approximation. The FHNC integral equations are used to sum terms involving f_c, while the SOC integral equations sum terms containing $f_{p=2,6}$. The accuracy and convergence of this method for simple potentials like Reid v_6 has been studied and found to be quite good.[13]

The L-dependent components of the potential and the $\mathbf{L}\cdot\mathbf{S}$ correlations are treated less generally, primarily at the two- and three-body level, because of the difficulty of chaining gradient operators. The treatment of $\mathbf{L}\cdot\mathbf{S}$ terms is described in Ref. 14, while the $v_{p=9,14}$ contributions are discussed in Ref. 2. One improvement in the results presented here compared to Ref. 2 is that a complete set of three-body separable diagrams containing $v_{p=9,14}$ and $f_{p=1,6}$ has been calculated, rather than selected samples as reported for diagrams 1.3—1.5 in Table 2 of Ref. 2. The accuracy of the treatment of L-dependent terms has not been thoroughly tested; the present comparison with Brueckner-Bethe results is probably the best test to date.

Another test of the accuracy of the FHNC—SOC summations in nuclear matter has been made for the first time in the present work by computing the energy expectation value with both the Pandharipande-Bethe (PB) and Jackson-Feenberg (JF) forms[15] of the kinetic energy. The kinetic energy may be written equivalently as:

$$\begin{aligned}-\hbar^2/2m\int d^3\tau\,\psi_v^*(\nabla_i^2\psi_v)&\\ =-\hbar^2/8m\int d^3\tau[\psi_v^*(\nabla_i^2\psi_v)&\\ +(\nabla_i^2\psi_v^*)\psi_v-2\nabla_i\psi_v^*\cdot\nabla_i\psi_v]\ .&\end{aligned}\tag{14}$$

The left-hand side is the PB form and leads to an energy expression

$$E_v(\mathrm{PB})=T+W+W_F+U+U_F\ , \tag{15}$$

where T is the one-body (Fermi gas) kinetic energy, W is a two-body integral containing both the potential V_{ij} and kinetic $\nabla_i^2F_{ij}$ terms, U is a three-body integral for $\nabla_iF_{ij}\cdot\nabla_iF_{ik}$ terms, and W_F and U_F are two- and three-

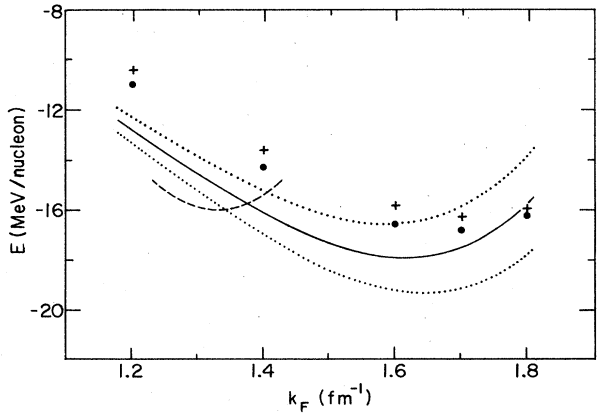

FIG. 1. Nuclear matter energy as a function of Fermi momentum. The solid line is fit to the Brueckner-Bethe energies; dotted lines show their estimated uncertainty. The dots and crosses show the variational JF and PB energies, respectively.

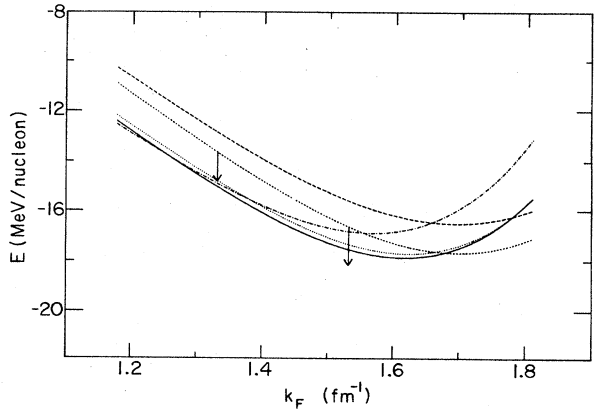

FIG. 2. Nuclear matter energy for four recent nucleon-nucleon potentials. The solid, dot, and dash-dot curves are fit to Brueckner-Bethe energies for the Argonne v_{14}, Paris, and Bonn potentials, while the long-dash and short-dash curves are fit to variational energies for the Argonne v_{14} and Urbana v_{14} potentials, respectively. The two vertical arrows show the effect of correlated basis function perturbation corrections on the Urbana v_{14} variational energy.

TABLE VIII. Contributions in MeV/nucleon to the variational PB energy for the Argonne v_{14} potential.

k_F (fm^{-1})	1.2	1.4	1.6	1.7	1.8
T	17.92	24.39	31.85	35.96	40.31
W (potential)	−43.72	−59.72	−78.24	−87.60	−97.25
W (kinetic)	17.12	23.52	31.66	36.28	40.35
W_F	−2.67	−3.68	−5.44	−7.00	−8.43
U	0.14	0.38	1.48	2.56	4.34
U_F	0.79	1.48	2.83	3.48	4.70
E_v (PB)	−10.42	−13.63	−15.86	−16.32	−15.98

body integrals for $\nabla_i F_{ij}\cdot\nabla\phi$ terms. The right-hand side is the JF form and leads to an energy expression[16]

$$E_v(\mathrm{JF}) = T + W_B + W_\phi + U_\phi \ , \tag{16}$$

where W_B is a two-body integral containing V_{ij} and $F_{ij}(\nabla_i^2 F_{ij}) - (\nabla_i F_{ij})^2$ terms, and W_ϕ and U_ϕ are two- and three-body kinetic energy integrals for $\nabla_i^2 |\phi|^2$ terms. The W, W_F, W_B, and W_ϕ integrals require knowledge of the pair-distribution function $g_2(r_{ij})$, while the U, U_F, and U_ϕ integrals require knowledge of the three-body distribution function $g_3(r_{ij},r_{jk},r_{ki})$. The U_ϕ of the JF form is extremely small (0.02 MeV at 1.8 fm^{-1}) compared to the U and U_F terms of the PB form (9 MeV at 1.8 fm^{-1}), so it is less sensitive to errors in approximating g_3. However the W_B term in E_v(JF) is more sensitive to details of g_2 than the W term in E_v(PB), particularly at short distances where the potential is repulsive.

If the two- and three-body distribution functions were computed exactly, the PB and JF forms would be exactly equal. In the present case the two forms agree extremely well; the JF form gives 0.25 to 0.75 MeV more binding than the PB form for the densities studied. This close agreement is in sharp contrast to the case of liquid helium, where the JF form gives significantly less binding than the PB form in the FHNC approximation.[15] (Physically, this is because nuclear matter is a much less dense system, with the core of the nucleon-nucleon interaction taking a much smaller fraction of the volume than the core of the atom-atom interaction in liquid helium.)

The variational calculation was repeated ~15 times for each density, with different values for the parameters d, d_t, and α. A least squares fit to the most general quadratic in d, d_t, and α was then used to find the optimal set of these parameters; they are given in Table VII. The PB energy and its contributions are given in Table VIII, while the JF energy and its corresponding pieces are given in Table IX. The W term of Eq. (15) and the W_B term of Eq. (16) include both the two-body potential energy and a kinetic energy piece; these are given separately.

IV. RESULTS AND DISCUSSION

The Brueckner-Bethe and variational results for Argonne v_{14} are shown in Fig. 1. The solid line is a fit to the Brueckner-Bethe energies, while the dotted lines on either side are fits corresponding to the estimated uncertainties given in Table IV. The circles and crosses show the variational JF and PB energies, respectively. The uncertainty in the variational energy expectation values is comparable to that in the Brueckner-Bethe calculations, being relatively small at low densities, and increasing with density. The dashed line shows the empirical saturation curve with a binding of 16 MeV at 1.33 fm^{-1} and an incompressibility of 210 MeV.

The variational energies are above the Brueckner-Bethe energies up to ~1.8 fm^{-1}, where the calculational uncertainties are much larger than the difference between the two calculations. The variational calculation gives a saturation point that is ~0.1 fm^{-1} higher in density than the Brueckner-Bethe calculation. At the lowest densities, the variational results are 2 MeV above the Brueckner-Bethe energies, while the sum of the estimated uncertainties is only 1 MeV. This difference probably reflects an inadequacy in the variational ansatz for the wave function. Possible improvements could include L^2 and $(\mathbf{L}\cdot\mathbf{S})^2$ correlations, or an explicit momentum dependence of the Feynman-Cohen backflow type.[16] Alternatively, perturbation corrections to the variational energy can be made using the correlated basis function approach.[17]

The differences between the results of the Brueckner-

TABLE IX. Contributions in MeV/nucleon to the variational JF energy for the Argonne v_{14} potential.

k_F (fm^{-1})	1.2	1.4	1.6	1.7	1.8
T	17.92	24.39	31.85	35.96	40.31
W_B (potential)	−43.72	−59.72	−78.24	−87.60	−97.25
W_B (kinetic)	16.19	22.78	32.17	37.73	44.00
W_ϕ	−1.39	−1.76	−2.39	−2.91	−3.32
U_ϕ	0.00	0.00	0.01	0.02	0.02
E_v (JF)	−11.00	−14.31	−16.60	−16.80	−16.24

TABLE X. Breuckner-Bethe (E_{BB}) and/or variational (E_v) binding energies in MeV/nucleon for four recent nucleon-nucleon potentials. The estimated uncertainty in E_{BB} is also given. The E_v are the average of JF and PB energies, while E_v(PB)-E_v(JF) is given in parentheses.

k_F (fm^{-1})	1.2	1.4	1.6	1.7	1.8
Bonn E_{BB}	−12.9±0.5	−15.9±0.7	−16.8±1.1		−13.5±1.9
Paris E_{BB}	−12.6±0.5	−15.9±0.8	−17.7±1.1		−15.8±1.8
Argonne v_{14} E_{BB}	−12.8±0.5	−16.2±0.9	−17.8±1.3		−15.8±2.0
Argonne v_{14} E_v	−10.7(0.6)	−14.0(0.7)	−16.2(0.7)	−16.6(0.5)	−16.1(0.3)
Urbana v_{14} E_v	−11.3(0.4)	−14.8(0.5)	−17.3(0.3)	−17.7(0.0)	−17.2(−0.5)

Bethe and variational calculations for Argonne v_{14} are very similar to the differences between the earlier results for Reid v_6. The reasonably good agreement between the two methods has been preserved with the addition of the $\mathbf{L}\cdot\mathbf{S}$, L^2, and $(\mathbf{L}\cdot\mathbf{S})^2$ terms to the potential. This is despite the less complete treatment afforded these terms, compared to the v_6 terms, in the variational calculations.

The results of Brueckner-Bethe and/or variational calculations for four recent potentials are summarized in Table X and Fig. 2. The solid, dot, and dash-dot lines in Fig. 2 show Brueckner-Bethe energies for the Argonne v_{14}, Paris, and Bonn potentials, respectively. The long-dash and short-dash lines show the average of the PB and JF variational energies for Argonne v_{14} and Urbana v_{14}, respectively. The Brueckner-Bethe saturation points for Paris and Bonn were reported previously;[1] the full saturation curves are given here. The estimated uncertainty in E_{BB} for these potentials is similar to that for Argonne v_{14} given in Table IV. Variational calculations for Urbana v_{14} were also reported earlier;[2] the present results reflect the improvements in the calculation discussed above.

Fantoni, Friman, and Pandharipande[17] have reported correlated basis function perturbation corrections to the Urbana v_{14} variational energy of −1.2 MeV at 1.33 fm^{-1} and −1.5 MeV at 1.53 fm^{-1}. These corrections are shown as vertical arrows in Fig. 2, and bring the Urbana v_{14} results into close agreement with the Brueckner-Bethe curves in the region of the empirical saturation density. If the perturbation correction to Argonne v_{14} were about the same, all the binding energy curves would be in remarkably close agreement.

All the potentials considered here give good fits to two-nucleon scattering data and deuteron properties. As seen in Fig. 2, all give too high a saturation density. While the calculated saturation point depends on the potential and on the calculational method, the contribution of the two-nucleon potential to the nuclear matter binding energy in the empirical saturation region seems to be well established. Clearly an additional effect, such as the addition of a three-nucleon potential to the nuclear Hamiltonian,[10,18] is required to obtain the empirical saturation properties.

This work was supported by the U.S. Department of Energy under Contract No. W-31-109-ENG-38.

*Present address: AT&T Bell Laboratories, Naperville, IL 60566.

[1]B. D. Day, Phys. Rev. Lett. **47**, 226 (1981).
[2]I. E. Lagaris and V. R. Pandharipande, Nucl. Phys. **A359**, 331 (1981); **A359**, 349 (1981).
[3]V. R. Pandharipande and R. B. Wiringa, Rev. Mod. Phys. **51**, 821 (1979).
[4]R. V. Reid, Ann. Phys. (N.Y.) **50**, 411 (1968).
[5]B. D. Day, Phys. Rev. C **24**, 1203 (1981).
[6]R. B. Wiringa and V. R. Pandharipande, Phys. Lett. **99B**, 1 (1981).
[7]R. B. Wiringa, R. A. Smith, and T. L. Ainsworth, Phys. Rev. C **29**, 1207 (1984).
[8]M. Lacombe, B. Loiseau, J. M. Richard, R. Vinh Mau, J. Cote, P. Pires, and R. de Tourreil, Phys. Rev. C **21**, 861 (1980).
[9]K. Holinde and R. Machleidt, Nucl. Phys. **A247**, 495 (1975).
[10]J. Carlson, V. R. Pandharipande, and R. B. Wiringa, Nucl. Phys. **A401**, 59 (1983); R. B. Wiringa, *ibid.*, **A401**, 86 (1983).
[11]B. Friedman and V. R. Pandharipande, Nucl. Phys. **A361**, 502 (1981).
[12]B. D. Day, in *From Nuclei to Particles: Proceedings of the International School of Physics "Enrico Fermi", Course LXXIX*, edited by A. Molinari (North-Holland, Amsterdam, 1981).
[13]R. B. Wiringa, Nucl. Phys. **A338**, 57 (1980).
[14]I. E. Lagaris and V. R. Pandharipande, Nucl. Phys. **A334**, 217 (1980).
[15]J. G. Zabolitzky, Phys. Rev. A **16**, 1258 (1977).
[16]E. Manousakis, S. Fantoni, V. R. Pandharipande, and Q. N. Usmani, Phys. Rev. B **28**, 3770 (1983).
[17]S. Fantoni, B. Friman, and V. R. Pandharipande, Nucl. Phys. **A399**, 51 (1983).
[18]R. Schiavilla, V. R. Pandharipande, and R. B. Wiringa, University of Illinois Report ILL-(NU)-85-40, 1985.